ATLAS-BASED CLUSTERING OF SULCAL PATTERNS – APPLICATION TO THE LEFT INFERIOR FRONTAL SULCUS

Olivier Coulon[1], *Vladimir Fonov*[2], *Jean-François Mangin*[3], *D. Louis Collins*[2]

[1]Aix-Marseille Univ, LSIS, UMR CNRS 6168, Marseille, France
[2]McConnell Brain Imaging Center, Montreal Neurological Institute, McGill University, Montreal, Canada
[3]CEA, I2BM, DSV, Neurospin, LNAO, Gif-sur-Yvette, France

ABSTRACT

We present an attempt at characterizing local patterns of cortical folding, an open problem in neuroscience. The technique is applied to an extremely variable sulcus: the left inferior frontal sulcus (LIFS). Our approach is based on the use of an average template as a reference to define features that characterize the position, presence, and orientation of elementary sulcal elements of the LIFS. Clustering was performed on the resulting feature vectors after the optimal number of clusters was found using the Gap statistic. The technique was applied to data from 151 subjects. Here, we present our results and discuss the nature of sulcal organization that exists within the apparently unstructured sulcal variability. ***Index Terms—***

Cortical folds, Clustering, Atlas

1. INTRODUCTION

Cortical organization is an open problem in neuroscience. Little is known about the organization of the cortical folding pattern and its link with development and function. Nevertheless, it has been hypothesized that this pattern has a specific geometric structure [1][2], and models of organization have been presented and tested [3]. In particular, the hypothesis of an orthogonal organization of the cortical folds around specific sulcal entities has emerged. The existence of such an organizational scheme is of great interest because of its potential relationship to brain function and because it is believed that many brain-related pathologies such as autism and epilepsy may be associated with disruptions of this scheme.

Gaining an understanding of cortical variability and organization first requires identification of the possible patterns for a specific fold or set of folds. The idea that a population can be divided into subgroups, with each member fitting a possible local pattern, has been used in the automatic labeling of cortical structures in [5]. Essentially, each local cortical component can be identified in a catalogue, and the global cortical organization is a collection of these local configurations. To explicitly describe local libraries of cortical patterns, large groups of subjects must be clustered in consistent subgroups, similar to what was done manually in [8]. Such a clustering approach has been performed in [6][7] using global shape descriptors or direct intersubject distances using the Iterative Closest Point (ICP) algorithm. Although the latter produces clear clusters for a few sulci, the global intersubject distance forces the use of either sulci with simple topological variations (e.g., the superior temporal sulcus) or larger sulcal sets with large-scale intergroup differences that can be captured by the global ICP-based distance (e.g., intermediate+marginal+orbital+inferior frontal region).

In the following, we present an attempt to characterize the folding patterns and fine local variability of a specific sulcus with extremely variable topography, the left inferior frontal sulcus (LIFS). This sulcus is of particular interest as one of the key boundaries of Broca's area, and existing cortical folding patterns could be related to functional specificities of the language system. Pattern characterization is achieved by clustering typical configurations after comparison with an unbiased, statistically centered atlas template built from a large set of subjects. Inspired by the notion of orthogonal directions presented in [1], namely, that variability occurs around two main orthogonal directions, our approach is based on the definition of features that measure the distances and orientations of individual LIFSs with reference to the template. Indeed, two main orthogonal directions are observable on the template LIFS. In parallel to the clustering process, we also investigated whether there was discernible structure within the variability, and in particular, whether clusters were present.

2. METHODS

2.1. Template extraction

We used the publicly available asymmetric version of the ICBM 2009c nonlinear average template[1] [9], which was created from 152 subjects in the International Consortium for Brain Mapping (ICBM) database. The template was processed with the BrainVisa T1 segmentation pipeline[2]. The white matter surface was extracted, and a complete representation of its folding pattern was constructed into a relational graph (Fig. 1). That it was possible to process this template through a pipeline dedicated to T1-weighted images is particularly striking: despite being the average of a large number of subjects, this template has a very well-defined morphology,

[1]http://www.bic.mni.mcgill.ca/ServicesAtlases
[2]http://brainvisa.info

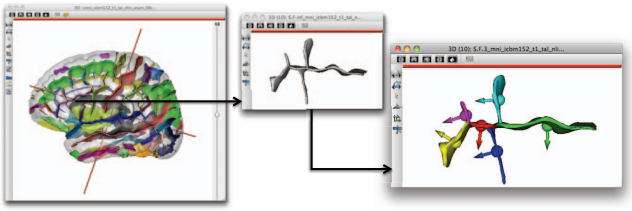


Fig. 1. The ICBM 2009c nonlinear asymmetric template. Left: White matter surface with sulci; Top right: Left inferior frontal sulcus; Bottom right: Six elementary pieces with $(c_i, \mathbf{d}_i)$.

as shown in Fig. 1. This property makes the template an ideal reference for studying cortical organization.

The template LIFS was then extracted as a triangular mesh and divided into six elementary pieces as shown in Fig. 1. Each piece $i = 1...6$ was then characterized by its position, that is, its center of gravity c_i and orientation $\mathbf{d}_i$, defined as the third eigenvector of a principal component analysis of the piece's mesh node coordinates. All $(c_i, \mathbf{d}_i)$ are shown in Fig. 1. As can be seen in the figure, pieces of the template LIFS roughly define two main folding directions, and the average template LIFS seems to show a complete folding pattern that includes all possible folds along those two directions.

2.2. Subjects and feature computation

We used T1-weighted magnetic resonance images (spoiled gradient sagittal acquisition, TE=10 ms, TR=18 ms, flip angle=30 °, 1×1×1 mm resolution) from 151 healthy young subjects acquired on a 1.5T Philips Gyroscan. Subjects were processed with the BrainVisa T1 segmentation pipeline. Automatic sulcal recognition was then applied [10], and the LIFS of each subject was automatically extracted as a three-dimensional (3D) mesh. For each LIFS, features were then computed as follows (see Fig. 2):

- The 3D LIFS mesh is non-linearly transformed to the average template space to remove unnecessary variability—such as size, global orientation, and, to some extent, geometry—while preserving the relevant characteristics: topology, local relative orientations, and local geometry.
- For each $i = 1...6$, p_i is the mesh node closest to c_i in the template space, and the distance feature $l_i = d_e(c_i, p_i)$ is computed, where d_e is the Euclidean distance. The normal direction $\mathbf{n}_i$ to the LIFS at p_i is determined (to be robust to noise and local geometric variation, $\mathbf{n}_i$ is regularized by averaging all normal directions in a second-order neighborhood). Finally, the directional feature $s_i = \mathbf{d}_i.\mathbf{n}_i$ is calculated.

Each LIFS is then characterized by 12 features: 6 distances (l_i), and 6 directionals (s_i). All features are computed for the

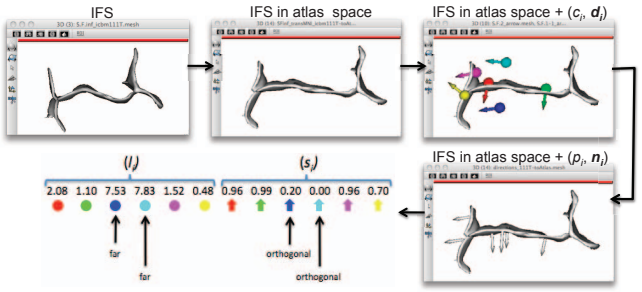


Fig. 2. Feature computation

151 subjects. The features are designed to estimate the presence and orientation of sulcal pieces with respect to the template. In the example shown in Fig. 2, two pieces are missing as indicated by the 'far' and 'orthogonal' feature values.

2.3. K-medoids clustering

2.3.1. *Algorithm*

To cluster the data, we used the K-medoids algorithm [11], a robust variant of the well-known K-means algorithm. In K-medoids, a centroid is chosen to represent each cluster, where a centroid is defined as the vector that minimizes the distance to all other vectors in the cluster. The algorithm is applied with the squared Euclidean distance and returns K clusters with their centroids. Before clustering, features are normalized such that the six distance and six orientational features have unit standard deviation across samples. Normalization is performed globally on each category (distance and orientation) to preserve the property that some features show greater variability than others within a category.

2.3.2. *Selecting the optimal number of clusters*

Applying a clustering algorithm such as K-medoids to any dataset will result in K clusters, even if the dataset has no structure (e.g., it is randomly sampled in a uniform distribution). If there are clusters in the data, determining their number is not a trivial task. Many methods have been proposed for estimating the number of clusters in a dataset (e.g., see [12]). Amongst these, the Gap statistic [13] has shown good performance not only in estimating the number K, but also in detecting the absence ($K = 1$) of clusters. This statistical approach essentially compares the data with a null reference distribution. For k clusters $(C_r)_{r=1...k}$ of size n_r, if $d_{ii'}$ is the squared Euclidean distance between items i and i', define:

$$D_r = \sum_{i,i' \in C_r} d_{ii'} \quad \text{and} \quad W_k = \sum_{r=1}^{k} \frac{1}{2n_r} D_r, \qquad (1)$$

where W_k is the pooled within-cluster sum of squares around the cluster means. The idea is then to compare $\log(W_k)$ with the value expected with a null reference distribution of the

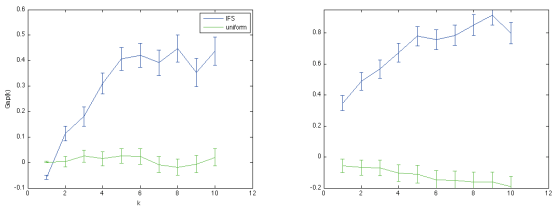


Fig. 3. Gap statistic as a function of the number of clusters, with the reference null distribution sampled by permutation of the original (left) and by bootstrap in a uniform distribution (right), on the LIFS data (blue) and for samples drawn in a uniform distribution (green). Error bars represent $\pm s_k$.

data. The Gap statistic is therefore defined as

$$\text{Gap}_n(k) = E_n^*\{\log(W_k)\} - \log(W_k), \qquad (2)$$

where $E_n^*\{\log(W_k)\}$ is the value expected with a sample of size n from the reference distribution. For K well-separated clusters, $\log(W_k)$ is expected to decrease faster than its expected rate for $k \leq K$ and slower than for $k > K$ [13]. The Gap statistic should then reach its maximum for $k = K$.

The choice of the reference distribution is important, and its variance structure particularly so. We generated each feature of the reference distribution by permutation of the observed values of the same feature in our data. This permutation resampling was performed $B = 2000$ times to estimate $E_n^*\{\log(W_k)\}$. To ensure the independence to our reference distribution, we also generated the features by drawing them uniformly over the range of observed values for that feature and then performing a bootstrap resampling B times.

When clusters are not so well separated (e.g., because of noise) or the structure is not trivial (e.g., a hierarchy of clusters), the choice of K is not as simple as merely taking the maximum of the Gap curve. If $\text{sd}(k)$ denotes the standard deviation of $\log(W_k)$ across the B reference distribution replicates, then, to account for the simulation error, we define $s_k = \sqrt{(1+1/B)}\text{sd}(k)$. The usual criterion for choosing K is then the smallest k for which $\text{Gap}(k) \geq \text{Gap}(k+1) - s_{k+1}$ [13].

3. RESULTS

The $\text{Gap}(k)$ curve was computed for the LIFS data with the two different reference distributions. Results are shown in Fig. 3 (in blue). To illustrate the ability of the Gap statistic to show structure and determine whether clusters were present in the data, we also generated a dataset with no clusters drawn randomly in a uniform distribution and computed the same $\text{Gap}(k)$ curve (in green). For both reference distributions, the curve clearly indicates an optimal number of clusters, $K = 5$, with a rapid increase of the Gap statistic up to this value.

We therefore applied the K-medoids algorithm to the LIFS feature data for the 151 subjects with $K = 5$. Each cluster included a number of subjects as follows: $|C_1| = 37$, $|C_2| = 29$, $|C_3| = 34$, $|C_4| = 39$, $|C_5| = 12$. On Fig. 4, isosurfaces of statistical probabilistic anatomy maps in the template space (known as SPAM) are shown for each cluster. It is clear on this figure how all clusters show a dominance of the rostrocaudal and dorsoventral directions. Clusters seem to be defined by their organization along those two directions, promoting the idea that cortical folding is organized according to an orthogonal system [1]. Morover, it is striking that each cluster's most probable configuration looks like a combination of several of the 6 atlas elementary pieces. Corresponding combinations of the template are shown on the middle row in Fig. 4. This also promotes the idea that the LIFS folding patterns are defined within a catalogue with a finite number of elements that define subgroups in the population. The template LIFS includes all possible patterns in this catalogue.

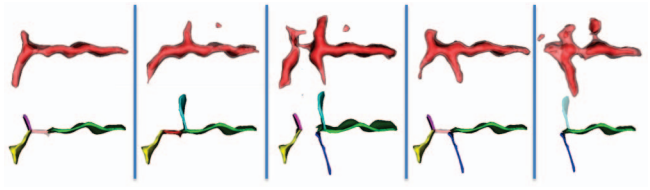


Fig. 4. row 1: clusters SPAM isosurfaces, rows 2: corresponding template combination. From left to right: Clusters 1 to 5.

In order to estimate the significance of each cluster, we computed a p-value based on a compactness index of each C_k, in a non-parametric way. Compactness, defined as the ratio of the average within-cluster distance to the average between-cluster distance, measures how well a cluster is separated from the rest of the data and should be optimized by the clustering algorithm. The dataset was resampled by permutation, and, for each resampling replicate, the K-medoids algorithm was applied and compactness was computed for the resulting five clusters. By resampling 2,000 times, we obtained 10,000 measures of compactness. Rank analysis led to the following p-values for the five clusters: $p(C_1) = .0033$, $p(C_2) = .0004$, $p(C_3) = .0025$, $p(C_4) = .0538$, $p(C_5) = .1332$. C_1, C_2, and C_3 show very good significance, while C_4 is reasonable. C_5 has a small number of subjects and seems to show unusual patterns that perhaps need more subjects to be captured in full. Indeed, the distances to the centroid increase, with an average of 1.16 and a maximum of 5.01 when other clusters are less than 0.52 and 2.67, respectively. To attempt a visual representation of the data structure, we applied the Isomap algorithm [14] to our features, an algorithm that provides an optimal low-dimensional embedding. The 2D Isomap embedding is shown in Fig. 5. Although it is only a reduced representation of the data structure, the clusters we found are shown to be grouped, the particular nature of C_5 (magenta), which is grouped outside the structure defined by the other clus-

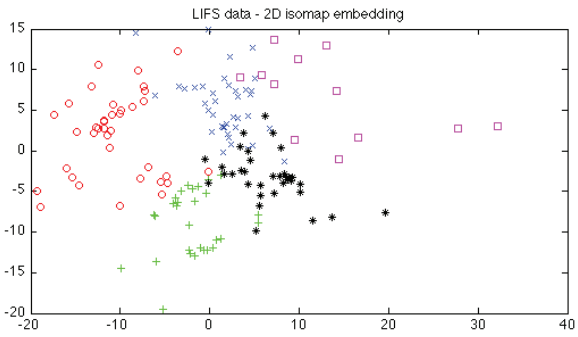


Fig. 5. Two-dimensional Isomap embedding of the LIFS data. Colors indicate which cluster each subject belongs to. Red: C_1; Green: C_2; Black: C_3; Blue: C_4; Magenta: C_5.

ters, is confirmed, and the proximity (with some form of a continuum) of C_3 and C_4 is visible.

The experiments demonstrate that structure exists within the high variability of sulcal folding patterns of the LIFS. More descriptive features may result in better classification of folding patterns. As shown in Fig. 2, where the LIFS includes the junction with the precentral sulcus, and in Fig. 4, where some of the LIFSs include parts of other sulci (intermediate frontal, orbital, and marginal sulci), the automatic labeling process produced some errors. The fact that our measurements are based on very local comparisons with the atlas LIFS makes the process somewhat robust against false positives (e.g., in Fig. 2, the inclusion of part of the precentral sulcus does not corrupt the measurements). False negatives, however, are still a problem; that is, the absence of a part of the LIFS will change the features. Moreover, robustness to labeling errors likely limits the possibility that our features are discriminative. For instance, it might be beneficial to include structural features of a more global nature, such as the number of connected components or principal orientations, although these features are more sensitive to labeling errors.

4. CONCLUSION

We have presented a method that automatically extracts consistent folding patterns to better describe the variability of the left inferior frontal sulcus. The use of a reference template provided an initial framework for analysis and allowed the definition of local features that can capture variability on a local scale. The nonlinear transformation to the template also helped to remove variability of non-interest. Future work will include the study of sulci labeled manually by an anatomist so as to avoid any extra variability introduced by labeling errors. More discriminative features also need to be defined for a clearer structure to be seen within such variable data, although applying the algorithm to less variable sulci should already prove beneficial. Ultimately, the description of local folding patterns is but one step toward understanding cortical variability and should be correlated with connectivity and functional information. Practically speaking, such an understanding will help to drive spatial normalization toward multi-template techniques and to identify biomarkers of developmental pathologies thought to be associated with perturbations in normal folding schemes.

Acknowledgements Olivier Coulon is funded by the *Agence nationale de la recherche* (ANR-09-BLAN-0038-01 'BrainMorph').

5. REFERENCES

[1] Régis, J, Mangin, J.-F., Ochiai, T., Frouin, V., Rivière, D., Cachia, A., Tamura, M., Samson, Y.: "Sulcal Root" Generic Model: a Hypothesis to Overcome the Variability of the Human Cortex Folding Patterns. Neurol Med Chir 45, 1–17 (2005)

[2] Toro, R., Burnod, Y.: Geometric Atlas: modeling the cortex as an organized surface. Neuroimage 20, 1468–1484 (2003)

[3] Clouchoux, C., Rivière, D., Mangin, J.-F., Operto, G., Régis, J., Coulon, O.: Model-driven Parameterization of the Cortical Surface for Localization and Inter-subject Matching. NeuroImage 50(2), 552–566 (2005)

[4] Klein, A., Mensh, B., Ghosh, S., Tourville, J., HIrsch, J.: Mindboggle: Automated brain labeling with multiple atlases BMC Medical Imaging 5(7) (2005)

[5] Sun, Z.Y., Rivière, D., Duchesnay, E., Thirion, B., Poupon, F., Mangin, J.-F.: Defining cortical sulcus patterns using partial clustering based on bootstrap and bagging. in ISBI 2008, 1629–1632 (2008)

[6] Sun, Z.Y., Perrot, M., Tucholka, A., Rivière, D., Mangin, J.-F.: Constructing a dictionary of human brain folding patterns in MICCAI 2009, 117–124 (2009)

[7] Ono, M., Kubuck, S., Abernathey, C.: Atlas of the Cerebral Sulci. Stuttgart, Georg Thieme Verlag (1990)

[8] Fonov, V., Evans, A.C., Botteron, K., Almli, C.R., McKinstry, R.C., Collins, D.L.: Unbiased average age-appropriate atlases for pediatric studies. NeuroImage 54, 313–327 (2011)

[9] Perrot, M., Rivière, D., Tucholka, A., and Mangin, J.-F.: Joint Bayesian Cortical Sulci Recognition and Spatial Normalization. In IPMI 2009, 176–187 (2009)

[10] Kaufman, L., Rousseuw, P.J.: Finding groups in data. Wiley series in probability and statistics, 1990.

[11] Gordon, A.: Classification. 2nd edition, London: Chapman and Hall (1999)

[12] Tibshirani, R., Walther, G., Hastie, T.: Estimating the number of clusters in a data set via the gap statistic. Journal of the Royal Statistical Society: Series B (Statistical Methodology) 63(2), 411–423 (2001)

[13] Tenenbaum, J., de Silva, V., Langford, J.: A global geometric framework for nonlinear dimensionality reduction. Science 290(5500), 2319–2323 (2000)